

Correlated forward-backward dissociation and neutron spectra as a luminosity monitor in heavy ion colliders

Anthony J. Baltz, Chellis Chasman, and Sebastian N. White*

Brookhaven National Laboratory, Upton, New York 11973

(January 12, 1998)

Abstract

Detection in zero degree calorimeters of the correlated forward-backward Coulomb or nuclear dissociation of two colliding nuclei is presented as a practical luminosity monitor in heavy ion colliders. Complementary predictions are given for total correlated Coulomb plus nuclear dissociation and for correlated forward-backward single neutrons from the giant dipole peak.

PACS: 25.75.-q; 29.40.Vj; 29.27.-a

keywords: Heavy ions; Calorimeter; Luminosity; Collider; Dissociation

I. INTRODUCTION

In a heavy ion collider such as RHIC the cross section for Coulomb dissociation of one of the ions in a $100 \text{ GeV} \times 100 \text{ GeV}$ Au + Au collision will be many times the geometric cross section, about 95 barns [1]. With such a large cross section available, it has been suggested that the correlated forward-backward Coulomb dissociation would provide a clean monitor of beam luminosity with the very forward (zero degree) calorimeters proposed for RHIC [2]. In fact the calculated cross section for mutual Coulomb dissociation was found to be quite large, about 4 barns. But there is an intrinsic limitation in the precision of

*Corresponding author. Tel.: 1-516-344-5488; fax: 1-516-344-3253; e-mail: white1@bnl.gov.

the calculated mutual Coulomb dissociation: a lower cutoff in impact parameter must be chosen, and the calculated mutual Coulomb dissociation varies approximately as the inverse square of this cutoff. However, it was found that if one adds nuclear dissociation to the mutual Coulomb dissociation calculation, the cutoff merges into the nuclear surface and the calculated cross section of 11 barns is relatively insensitive to parameter variation [3]. Details of these calculations are presented in Section III below.

The proposed zero degree calorimeter [4] detects the total neutral energy in the forward direction. For neutrons of the beam momentum the detected signal varies then as the number of neutrons. While the dissociation cross section includes excitations of the nucleus up to many GeV, the largest contribution is for excitations of less than about 25 MeV, the region of the giant dipole resonance, amounting to about 65 barns. Photonuclear data [5] indicate that the excited state decays predominantly by single neutron emission in this region; we will show that the Coulomb dissociation to a single neutron final state is large (50 barns) and contained in a single energy peak within about 10% of the beam energy. In Section IV we present details and consider the detection of correlated single neutron peaks.

Based on the above we will present several complementary methods of using calculations of mutual Coulomb plus nuclear dissociation along with zero degree calorimeter measurements as an absolute luminosity calibration at heavy ion colliders such as RHIC and LHC. But first we will begin with some experimental considerations.

II. EXPERIMENTAL CONSIDERATIONS

The primary quantities of interest are: (1) the luminosity, (2) the distribution and centroid of the interaction region along the beam direction, and (3) the distribution in time of the interactions relative to the nominal bunch crossing time. A basic requirement on the reaction chosen for these measurements (particularly of luminosity) is that it be relatively background free and that it have a straightforward acceptance, implying simple correction of measured rates for experimental details. Finally, if this reaction is to be used as an absolute

luminosity determination, it will be necessary to reduce uncertainties in the calculated cross section to $\leq 5\%$ or better. We deal below with the issues pertaining to luminosity. The other principal measurements rely on the timing resolution of the neutron detectors.

What is the rate from which luminosity is calculated? We propose to measure the coincidence rate requiring forward and backward energy of ≥ 60 GeV within 2 mrad of each beam direction. These requirements are largely chosen to minimize uncertainties in the calculated cross section. The coincidence requirement is also necessary to reduce contamination from background sources.

The 60 GeV threshold choice (assuming 100 GeV/u beam energy) is simply a requirement of at least 1 fragmentation neutron emitted into the detector and allows for linewidth and experimental resolution. (A resolution of $\leq 20\%$ at 100 GeV is expected for a practical detector). Since at a collider the forward direction is only accessible downstream of beam steering magnets, the contribution from protons and charged fragments is expected to be negligible [6,7]. Further specifics are detailed in the following.

A. Energy Threshold

In order to include a real energy threshold in the coincidence requirement we consider it essential that some fraction of triggers populate an energy peak which can be clearly resolved from the continuum. The peak will be used to adjust trigger energy scale and to compute inefficiencies after the fact. We examine below the energy spectrum of neutrons emitted in Coulomb dissociation. Single neutron emission turns out to be prominent because of the importance of the giant dipole resonance; the natural energy spread is smaller than the expected detector resolution.

B. Experimental Backgrounds

There are two principal types of experimental background that concern us, those from beam interactions (which are therefore proportional to luminosity) and those which arise

from single beam interactions with residual gas in the machine, for example, (and do not depend directly on luminosity). The coincidence requirement is designed to largely eliminate the latter.

Single beam rates can be estimated from the nominal conditions and vacuum requirements called for in the experimental areas. Beam gas rates are expected to be lower than the minimum bias interaction rate at full luminosity (i. e. the signal to be measured, roughly 7 barns cross section for Au on Au). Since the actual minimum bias rate can be significantly lower than the nominal design value during commissioning the beam gas rate could become significant. Similarly, rates due to interactions of the beam halo, which are difficult to calculate a priori, could also be a large background source.

The requirement of forward-backward coincidences greatly reduces the full counting rate due to these sources except for accidentals. It also makes possible the secondary measurements described above. The spatial distribution of interactions is calculated from forward-backward time differences. Assuming a time resolution of order 200 psec, we calculate a spatial resolution of a few cms. Backgrounds due to accidental coincidences between the two beam directions, including contributions from beam-beam interactions such as single beam Coulomb dissociation (95 barns at RHIC), are found to be negligible.

C. Luminosity Calibration and Cross section Uncertainties

As was indicated in the Introduction, mutual Coulomb dissociation calculations are probably limited to an uncertainty of not less than about 5%. There is a lower impact parameter cutoff in the Weizsacker-Williams formalism that has no clear experimental counterpart. In fact, it is difficult to define an experimental cut which would clearly distinguish between strong interaction final states and those that arise from the high energy component of the Weizsacker-Williams spectrum.

For this reason in Section III we examine the possibility of calculating a cross section which is actually the sum of Coulomb and nuclear processes leading to the forward-backward

coincidence of neutral beam energy clusters. We find that this almost completely eliminates the above uncertainties.

D. Beam Fragmentation in Nuclear Collisions

Before we perform this calculation of Coulomb plus nuclear dissociation we must address the question of the fraction of nuclear interactions, as a function of impact parameter, in which heavy ion collisions lead to a neutral beam energy cluster within 2 mr of the beam direction. Fortunately this measurement has been recently performed in a dedicated test at the CERN SPS [8]. For our purposes the probability of producing less than one neutral forward cluster, even in a central collision, is negligible. In what follows, we take the probability of a neutral beam energy cluster within 2 mr of the beam direction to be unity.

III. MUTUAL COULOMB PLUS NUCLEAR DISSOCIATION

The cross section for heavy-ion dissociation may be accurately expressed in terms of (generally experimentally known) photo-dissociation cross sections $\sigma_{ph}(\omega)$ of the same nucleus over an appropriate energy range of photon energies ω . This is the so-called Weizsacker-Williams expression

$$\sigma_{dis} = \frac{2\alpha Z_p^2}{\pi\gamma^2} \int d\omega \omega \sigma_{ph}(\omega) \int_{b_0}^{\infty} b db K_1^2\left(\frac{b\omega}{\gamma}\right), \quad (1)$$

where K_1 is the usual modified Bessel function. The lower cutoff of the impact parameter integral b_0 is normally fixed at a value to separate pure Coulomb excitation from nuclear processes. b_0 provides a somewhat arbitrary parameter dependence which we deal with below.

We may define a probability of dissociation, $P(b)$ as a function of impact parameter b

$$\sigma_{dis} = 2\pi \int_{b_0}^{\infty} P(b) b db. \quad (2)$$

Then inverting the order of integration in Eq. (1) we have

$$P(b) = \frac{\alpha Z_p^2}{\pi^2 \gamma^2} \int d\omega \omega \sigma_{ph}(\omega) K_1^2\left(\frac{b\omega}{\gamma}\right). \quad (3)$$

If we assume independence of the various modes of dissociation, then the probability of at least one dissociation excitation of the nucleus is given by the usual Poisson distribution. If the first order probability of Coulomb dissociation at a given impact parameter b is $P_C(b)$, then the probability of at least one mutual Coulomb dissociation $P_C^m(b)$ is given by

$$P_C^m(b) = (1 - e^{-P_C(b)})^2. \quad (4)$$

The corresponding probability of at least one mutual nuclear dissociation $P_N^m(b)$ is given in terms of a first order probability $P_N(b)$ by

$$P_N^m(b) = (1 - e^{-P_N(b)}). \quad (5)$$

Note that there is no square here; all nuclear dissociation is mutual. $P_N(b)$ is evaluated from the Glauber model:

$$P_N(b) = \int dx dy dz_p \rho_p(x - b, y, z_p) (1 - e^{\sigma_{NN} \int dz_t \rho_t(x, y, z_t)}). \quad (6)$$

The densities ρ_p, ρ_t are parameterized with a Fermi function. For Au the charge distribution parameters are $R_C = 6.38, a = .535$ fm [9]. From Hartree-Fock calculations one finds that the neutron radius should be a little larger [10]. We take the neutron radius of Au to be 6.6 fm and then average for a best overall radius of 6.5. At RHIC energies the total nucleon-nucleon cross section σ_{NN} is 50 mb [11].

Consider now the probability of survival without mutual Coulomb or nuclear dissociation $P_S(b)$. It is the product of the separate probabilities. Since all nuclear dissociation is mutual, the nuclear-Coulomb mutual dissociation contribution is redundant. We have

$$\begin{aligned} P_S(b) &= (1 - P_C^m(b))(1 - P_N^m(b)) \\ &= e^{-P_N(b)}(2e^{-P_C(b)} - e^{-2P_C(b)}). \end{aligned} \quad (7)$$

The probability of mutual excitation is then

$$P(b) = 1 - e^{-P_N(b)}(2e^{-P_C(b)} - e^{-2P_C(b)}). \quad (8)$$

Let us take the standard design case of 100 GeV + 100 GeV Au + Au at RHIC. Seen in the frame of the nucleus being dissociated, the equivalent γ of the other ion providing the equivalent photons is 23,000. The experimental photo-dissociation cross section $\sigma_{ph}(\omega)$ that we utilized is shown in Fig. 1, which we have taken from Ref. [1].

In Table I we present calculated first order and unitarity corrected mutual Coulomb dissociation cross sections for two values of b_0^2 , 2.25 barns and 3 barns, corresponding to r_0 values of 1.29 and 1.49 respectively when one expresses b_0 in term of $2 \times r_0 A^{1/3}$. Cross sections are tabulated as a function of a cutoff in ω , which should correspond in some fashion to an experimental acceptance. For comparison, the corresponding cross sections for 2.76 TeV + 2.76 TeV Pb + Pb collisions at LHC are shown in Table II.

Fig. 2 shows the calculated probabilities of correlated forward-backward dissociation as a function of impact parameter. At impact parameters of 13 fm and below the mutual dissociation probability becomes unity from the nuclear dissociation alone. Table III shows the parameter dependence of correlated dissociation cross sections. The first four rows show how the calculated mutual dissociation cross section becomes independent of the cutoff parameter for values less than about 15 fm. The fifth row compared to the second row shows how a small increase in the nuclear size parameter causes a small increase in the computed cross section. The sixth row shows how a 20% reduction in the nucleon-nucleon cross section leads to a less than 1% reduction in the mutual dissociation cross section. The overall conclusion is that we can predict a mutual Coulomb plus nuclear dissociation cross section of 11 barns with an error of less than about 5%.

IV. FORWARD-BACKWARD ENERGY PEAK

From Eq.(1) we can write down the differential Weizsacker-Williams cross section for heavy-ion dissociation

$$\frac{d\sigma_{dis}}{d\omega} = \frac{2\alpha Z_p^2 \omega}{\pi \gamma^2} \sigma_{ph}(\omega) \int_{b_0}^{\infty} b db K_1^2\left(\frac{b\omega}{\gamma}\right). \quad (9)$$

$\sigma_{ph}(\omega)$ is the photon cross section; in the present calculation we take it from the photo-dissociation data leading to only a single neutron in the final state [5]. The square of the Bessel function gives the the energy and impact parameter dependent number of equivalent photons from the heavy ion.

The impact parameter integral may be approximated very accurately for $b_0\omega \ll \gamma$ to yield

$$\int_{b_0}^{\infty} b db K_1^2\left(\frac{b\omega}{\gamma}\right) = \frac{\gamma^2}{\omega^2} \left[\ln\left(\frac{2\gamma}{b_0\omega}\right) - \gamma_{euler} - .5 \right] = \frac{\gamma^2}{\omega^2} \ln\left(\frac{.681\gamma}{b_0\omega}\right). \quad (10)$$

Putting in the factor of $\hbar c$ explicitly we obtain the familiar form

$$\frac{d\sigma_{dis}}{d\omega} = \frac{2\alpha Z_p^2}{\pi \omega} \sigma_{ph}(\omega) \ln\left(\frac{.681 \hbar c \gamma}{b_0 \omega}\right). \quad (11)$$

The energy dependence of the $(\gamma, 1n)$ cross section on Au [5], $\sigma_{ph}(\omega)$, is shown as the dashed line in Fig. 3. The Au + Au cross section for single neutrons in either forward beam direction, obtained from Eq. (11), is shown as the solid line in Fig. 3. Notes the difference in scale on the plot of the two cross sections. Setting the impact parameter cut off b_0 to 15 fm and integrating from the threshold at 8.1 MeV up to 24.0 MeV, we find that the Coulomb excitation to a single neutron final state, σ_{dis} , is 50.6 barns.

The angular distribution of neutrons emitted from the giant dipole resonance has been parameterized in the form $A + B \sin^2(\theta)$, and for Au A/B has been measured to be .58/.38 [12]. If one relativistically boosts the emitted soft neutron energy to the lab frame, then one obtains the spectra of Fig. 4. The solid line is the predicted spectrum from the experimental ratio of A/B . For comparison, a purely isotropic distribution (dot-dashed line) and a $\sin^2(\theta)$ distribution (dashed line) are also shown.

From Fig. 4 it is clear that no matter what the the angular distribution of the emitted neutrons is, there will be a huge one neutron peak of about 50 barns. Because of its size, this peak will stand out with very little background: other single neutron contributions from higher energy dissociation will be relatively negligible [13] [14]; soft two neutron

spectrometer contributions will be centered at about twice the single neutron energy of 100 GeV; higher numbers of neutral particles will be correspondingly higher in energy. Thus the large, well characterized single neutron peak provides an ideal component for a Au + Au beam luminosity monitor in the forward calorimeter at RHIC.

Now let us consider mutual Coulomb dissociation in which one or both of the reaction products is a single neutron at the beam momentum. The previous analysis made use of the lowest order expression Eq. (11) for the single neutron cross section which is not properly unitarized and contains a logarithmic dependence on b_0 . A more accurate expression may be obtained in analogy with Section III by again assuming a Poisson distribution in the number of excitations. Then the probability of one and only one neutron excitation $P_{1n}(b)$ may be expressed terms of the first order probability of one neutron excitation $P_{1n}^1(b)$ and the normalization factor $e^{-P_N(b)-P_C(b)}$ which involves all excitations

$$P_{1n}(b) = P_{1n}^1(b)e^{-P_N(b)-P_C(b)}. \quad (12)$$

Note that the normalization factor provides a natural impact parameter cutoff; we will not need a dependence on b_0 in our cross section expression Eq. (2). Multiple neutron final states completely dominate for impact parameters smaller than grazing.

The expression for mutual Coulomb dissociation in which both of the neutral reaction products are single neutrons is the square of the Eq. (12) expression. The analagous expression for mutual Coulomb dissociation in which one reaction products is a single neutron and the other is any excitation is

$$P_{1n,xn}(b) = P_{1n}^1(b)e^{-P_N(b)-P_C(b)}(1 - e^{-P_N(b)-P_C(b)}). \quad (13)$$

Table IV shows the dependence of computed cross sections on the radius parameter of the nuclear density. For Au + Au 6.38 corresponds to the the radius of the proton density while 6.50 is probably a more realistic value, an average between a proton density and an expected neutron density. In any case the dependences are not large. The mutual cross sections vary by about 1% over this range while the uncorrelated cross sections vary by less than a tenth of one per cent.

The correlated single neutron cross section is predicted to be .45 barns and the correlated cross section for a single neutron in one specified detector along with any neutral in the other (including possibly a single neutron) is three times that, 1.35 barns. For completeness the 11 barn cross section of Table III for any mutual excitation is repeated.

Corresponding cross sections for Pb + Pb at LHC have also been computed and are also displayed in Table IV. For Pb the charge distribution parameters are $R_C = 6.624$, $a = .549$ fm [9] and a more realistic nucleon matter radius is taken to be 6.65. At LHC energies the total nucleon-nucleon cross section σ_{NN} is taken to be 85 mb [11]. Again radius dependences are not large.

One might consider using the predicted 49 barn single neutron peak as a luminosity monitor. The limitation of this method comes from the luminosity independent backgrounds due to beam gas and beam halo interactions discussed in Section II. The 102 barn nuclear plus Coulomb dissociation cross section suffers from the same limitations without the positive energy signal of the neutron peak. Requiring a forward-backward single coincidence should largely eliminate these backgrounds with the experimental advantage of having at least one the neutron peaks.

V. Z DEPENDENCE

We have performed calculations involving mutual Coulomb dissociation for Au + Au and Pb + Pb reactions to exploit multi-barn cross sections. Unfortunately these large cross sections do not persist to collisions of lighter ion species: mutual dissociation cross sections scale approximately as Z^6 . This is because single Coulomb dissociation scales as Z^2 times the number of nucleons for the highest excitations or as Z^2 times $(NZ)/A$ for the giant dipole resonance. Table V presents some representative comparisons. Clearly for ions as light as Ca + Ca and O + O correlated forward-backward energy deposit will be dominated by purely nuclear collisions, and will lead to a simple geometric mutual cross section.

VI. DISCUSSION

We have presented several complementary solutions to using computed Coulomb dissociation as a luminosity monitor at RHIC (and LHC). As we showed in Section III, if we measure the combined Coulomb plus nuclear mutual dissociation cross section, then we eliminate the problem of the lower cutoff in the calculation of the mutual Coulomb dissociation cross section. The mutual Coulomb plus nuclear cross section is predicted to be 11 barns. This absolute theoretical prediction should be good to about 5% or better, but one must detect a signal for all mutual events regardless of energy. As we showed in Section IV, if we measure the neutron spectra, then we should find a clean peak from the giant dipole excitation in both directions. Requiring forward-backward coincidences within the one neutron peak at the beam energy gives a much smaller .45 barn cross section, but with the positive experimental energy identification of the beam momentum peaks. The other predicted cross sections in Table IV could provide complementary roles as a luminosity monitor, especially by exploiting their predicted ratios.

REFERENCES

- [1] A. J. Baltz, M. J. Rhoades-Brown, and J. Weneser, *Phys. Rev. A* **54**, 4233 (1996).
- [2] A. J. Baltz and S. N. White, RHIC/DET Note 20, BNL-67127 (1996).
- [3] A. J. Baltz and S. N. White, Summary of the 2nd Zero Degree Workshop at BNL, February 21-22, 1997.
- [4] Proposal to build Forward Calorimeters for the RHIC Heavy Ion Experiments, www.rhic.bnl.gov/html/zdc.html, August, 1997.
- [5] A. Veyssi re, H. Beil, R. Berg re, P. Carlos, and A. Lepr tre, *Nuc. Phys.* **A159**, 561 (1970).
- [6] RHIC Design Manual, BNL-52195 (1989).
- [7] Alice Technical Proposal, CERN/LHCC 95-71.
- [8] T. Alber et al. (NA49 collaboration), manuscript in preparation.
- [9] H. deVries, C. W. deJager, and C. deVries, *Atomic and Nuclear Data Tables* **36**, 495 (1987).
- [10] C. J. Batty, E. Friedman, and A. Gal, *Progress of Theoretical Physics Supplement* **117**, 227 (1994).
- [11] R. M. Barnett, et al., Particle Data Group, *Phys. Rev. D* **54**, 1 (1996).
- [12] Franca Tagliabue and J. Goldemberg, *Nuc. Phys.* **23**, 144 (1961).
- [13] A. Lepr tre, H. Beil, R. Berg re, P. Carlos, J. Fagot, A. de Miniac, and A. Veyssi re, *Nuc. Phys.* **A367**, 237 (1981).
- [14] P. Carlos, H. Beil, R. Berg re, J. Fagot, A. Lepr tre, A. de Miniac, and A. Veyssi re, *Nuc. Phys.* **A431**, 573 (1984).

FIGURES

FIG. 1. Photonuclear dissociation cross sections utilized for the Au + Au Coulomb dissociation calculations.

FIG. 2. Calculated mutual dissociation probabilities for Au + Au at RHIC.

FIG. 3. The dashed line is the $(\gamma,1n)$ cross section on Au taken from Ref. [5] up to 20 MeV and extrapolated to zero at 24 MeV; the units are .1 barns per MeV (the peak is at .52 barns). The solid line is the single neutron cross section for Au + Au at RHIC (in barns per MeV).

FIG. 4. Forward single neutron spectra for Au + Au at RHIC. The dot-dashed line corresponds to an isotropic neutron distribution, the dashed line to a $\sin^2(\theta)$ distribution, and the solid line to the experimentally measured distribution (see text).

TABLES

TABLE I. First order σ_{cd}^1 and unitarity corrected σ_{cd} (in barns) for Au + Au at RHIC as a function of the cutoff photon energy ω_{max} (in MeV). Calculations are presented for two values of the lower impact parameter cutoff (see text).

ω_{max}	σ_{cd}^1		σ_{cd}	
	$b_0 = 15$	$b_0 = 17.32$	$b_0 = 15$	$b_0 = 17.32$
25	1.65	1.23	1.31	1.04
103	1.99	1.49	1.55	1.24
440	3.10	2.32	2.29	1.84
2000	4.21	3.16	2.98	2.42
17840	5.12	3.84	3.50	2.86
∞	5.91	4.39	3.90	3.19

TABLE II. As in Table I, but for Pb + Pb at LHC.

ω_{max}	σ_{cd}^1		σ_{cd}	
	$b_0 = 15$	$b_0 = 17.32$	$b_0 = 15$	$b_0 = 17.32$
25	2.21	1.66	1.71	1.36
103	2.66	2.00	2.01	1.61
440	4.12	3.09	2.92	2.37
2000	5.58	4.19	3.76	3.09
17840	6.79	5.09	4.42	3.65
∞	12.75	9.45	7.15	6.02

TABLE III. Parameter dependence of correlated dissociation cross sections for Au + Au at RHIC. Units are fm and barns.

σ_{NN}	b_0	R	a	σ_N	σ_C	σ_{NC}
50	10.	6.38	.535	6.92	6.03	10.90
50	12.76	6.38	.535	6.92	4.77	10.90
50	15.	6.38	.535	6.92	3.92	10.74
50	17.32	6.38	.535	6.92	3.17	10.09
50	12.76	6.5	.535	7.09	4.77	11.01
40	12.76	6.5	.535	6.97	4.77	10.93

TABLE IV. Dependence various cross sections (in barns) on the radius of the nuclear density R .

R	Au + Au at RHIC		Pb + Pb at LHC	
	6.38	6.50	6.624	6.75
$\sigma_{1n,1n}$.449	.445	.537	.533
$\sigma_{1n,xn}$	1.364	1.349	1.897	1.881
$\sigma_{xn,xn}$	10.90	11.01	14.75	14.85
σ_{1n}	49.20	49.18	105.93	105.91
σ_{xn}	102.35	102.42	227.28	227.34

TABLE V. Single and mutual Coulomb dissociation scaling. Cross sections for Ca + Ca and O + O were simply scaled appropriately by Z^3 or Z^6 from the calculations for Au + Au at RHIC.

Units are barns.

	Single		Mutual	
	All	One Neutron	All	One Neutron
Au + Au	95.	49.	3.9	.45
Ca + Ca	1.5	.8	.001	.0001
O + O	.1	.05	.000004	.0000005

Photonuclear Absorption Cross Section

Au Target

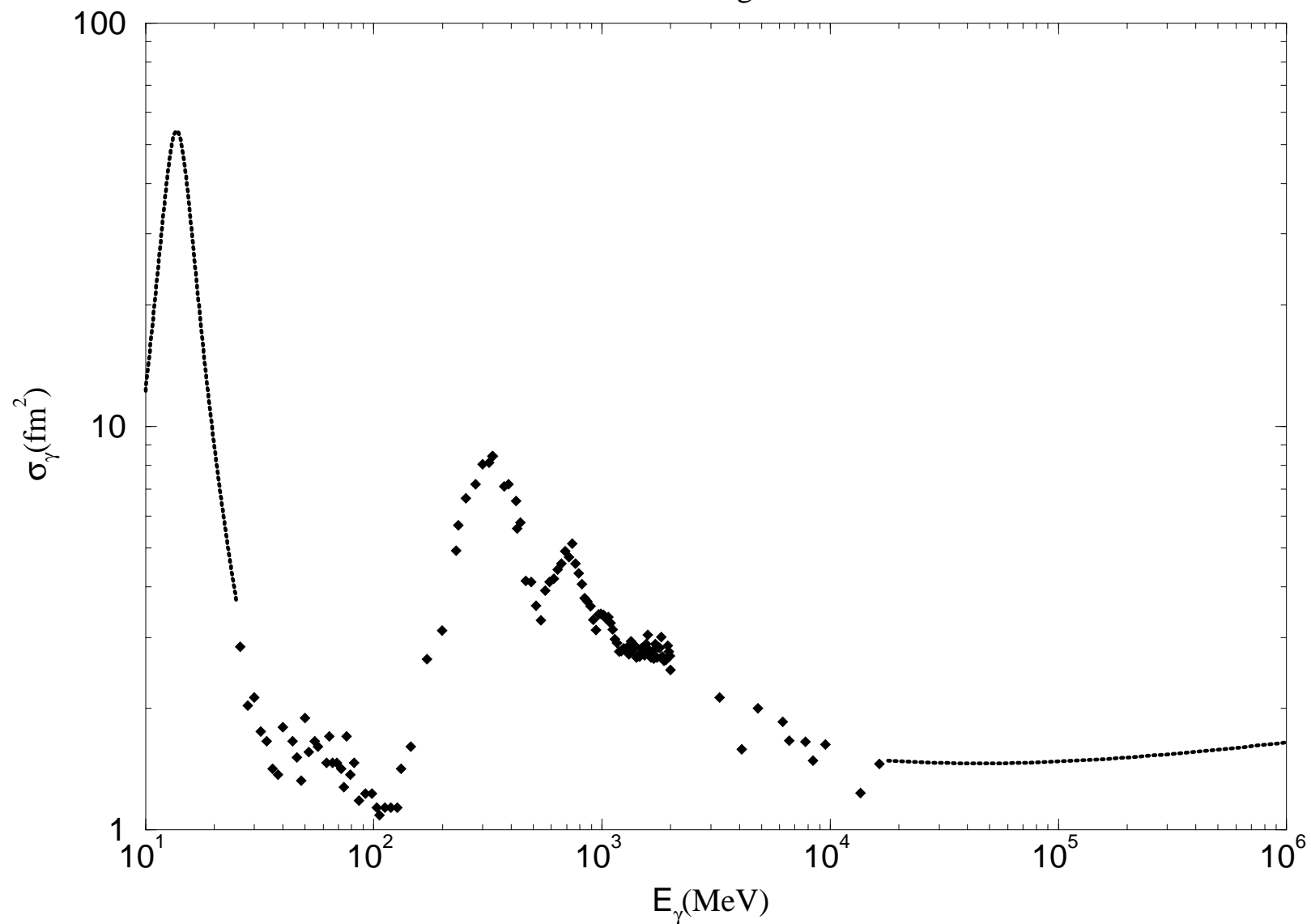


Fig 1

Correlated Forward-Backward Dissociation

Au + Au at RHIC

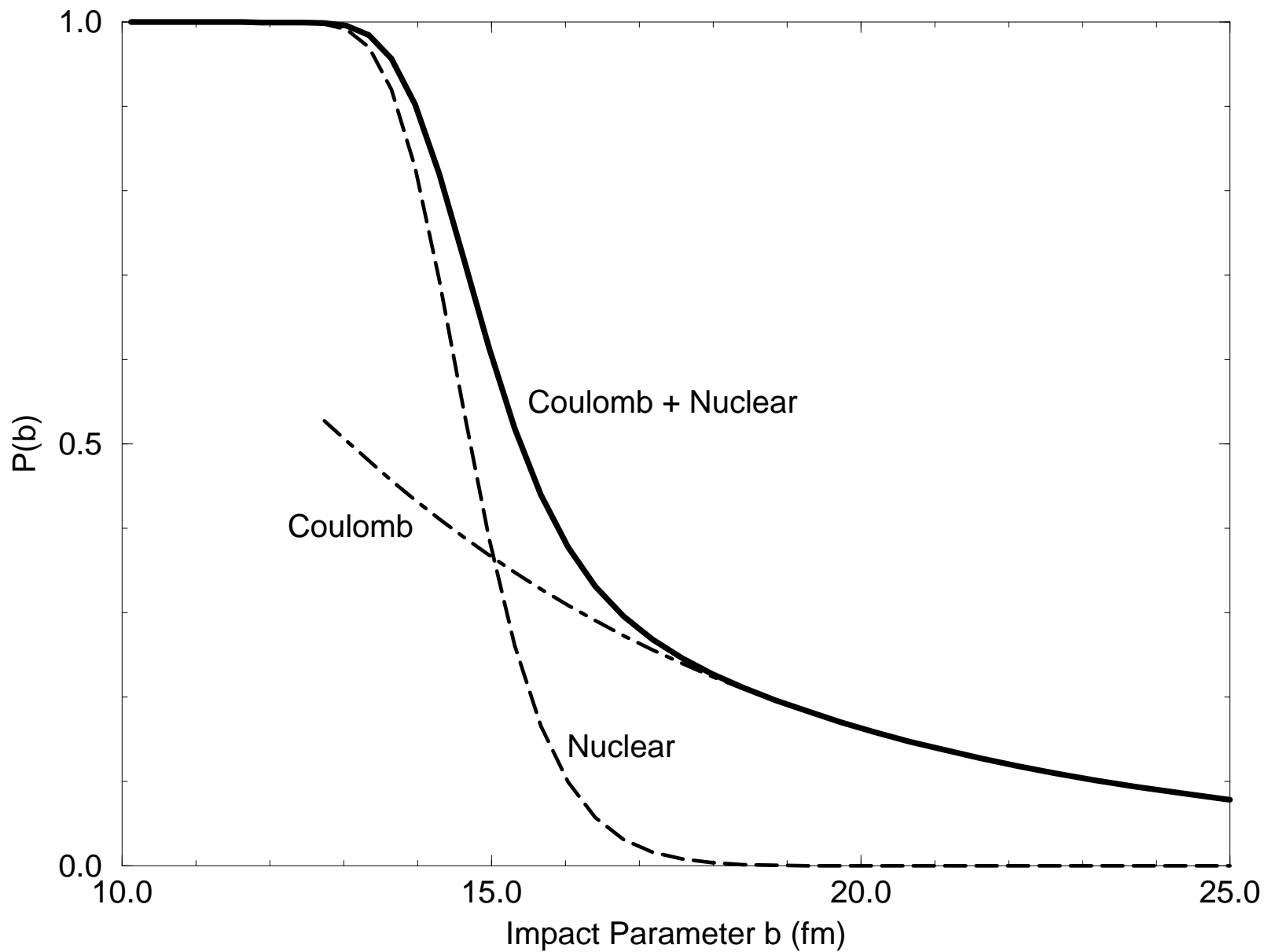


Fig. 2

Single Neutron Spectra

Au target

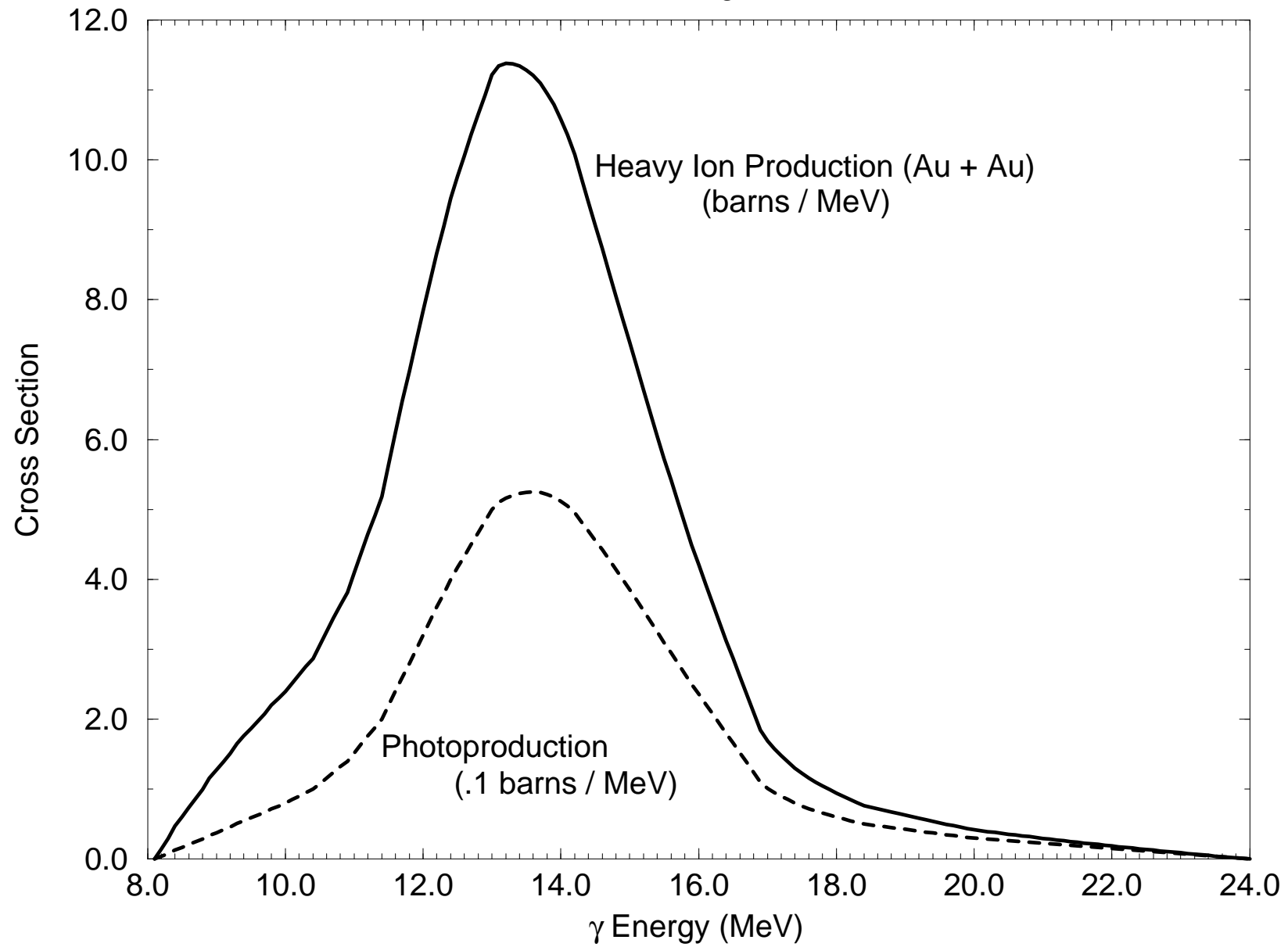


Fig. 3

Forward Single Neutrons

Au + Au

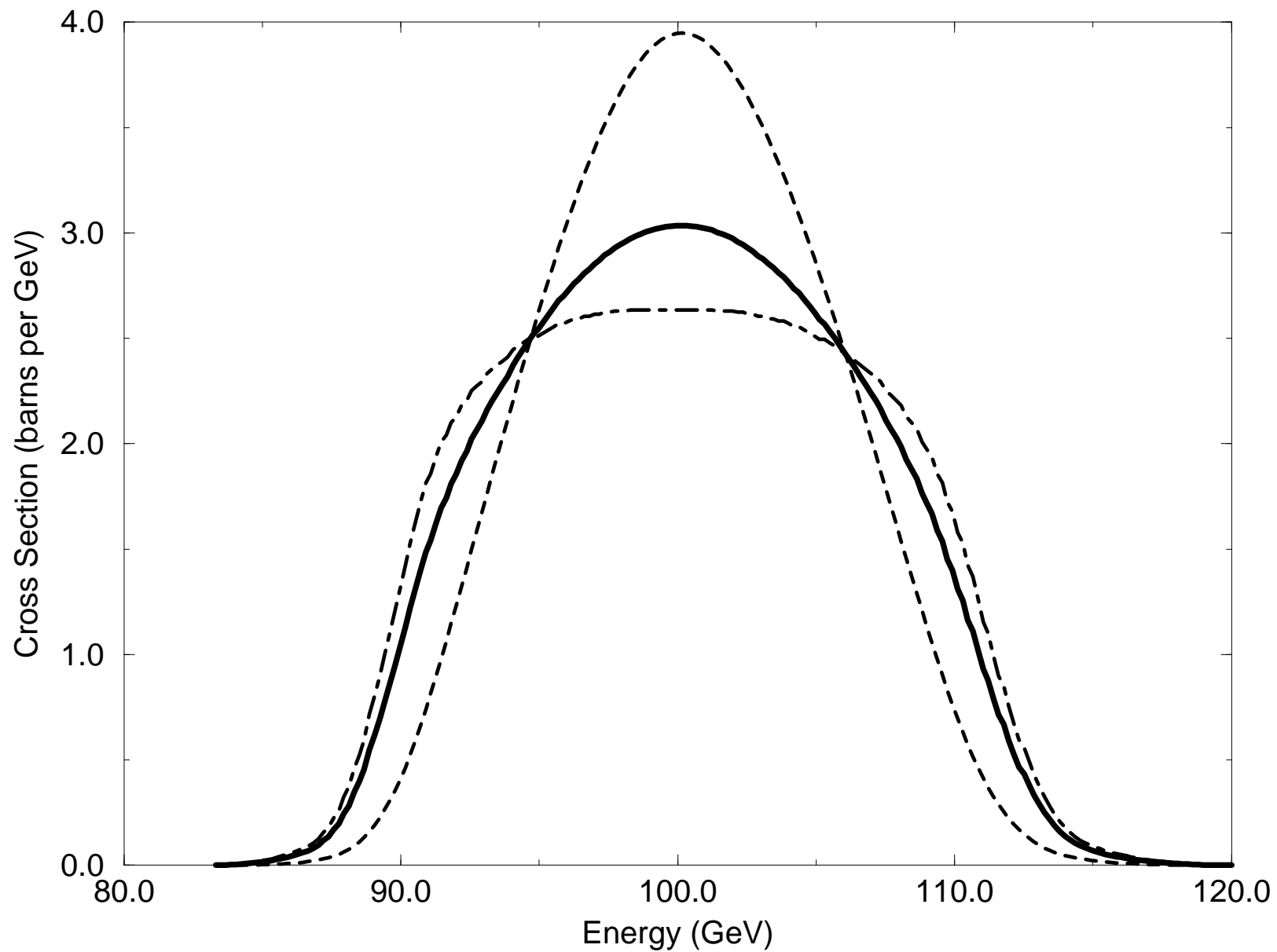


Fig. 4